

THE PHOTOCHEMISTRY OF CHROMIUM, MANGANESE,
AND IRON PORPHYRIN COMPLEXES

Kenneth S. Suslick* and Randall A. Watson

School of Chemical Sciences, University of Illinois at Urbana-Champaign, 505 S. Mathews Ave., Urbana, IL 61801, USA.

Received March 21, 1997, accepted July 28, 1997.

ABSTRACT. — A review is presented of the photochemistry of porphyrin complexes of the first row transition metals, particularly those of chromium, manganese, and iron. Their photochemistry has revealed a diverse set of reactions, including oxygen and nitrogen atom transfers, photoreductions, photooxidations, photocatalysis, and radical chain initiations. There is growing evidence that much of this diversity actually represents secondary thermal reactions. In many cases, the primary photoprocess is homolytic loss of an axial ligand, resulting in photoreduction of the metal and production of a reactive radical from the lost ligand. Subsequent fast thermal reactions can then lead to the formation of the wide range of reactivity observed. This observation is consistent with the nature of the excited states involved. Irradiation of the low energy $\pi \rightarrow \pi$ transitions does not produce photochemical reactions, and the observed photochemistry does not come from the lowest available excited state. Instead, the metalloporphyrin excited states that show photochemistry are those involved in charge transfer transitions, either from the axial ligand to the metal or from the porphyrin itself to the metal. Thus, the preponderance of metalloporphyrin photochemistry is observed in complexes with hyper spectra.

Introduction

Metalloporphyrins and related macrocycles serve many functions in biological systems. Their central role in charge separation as part of the photosynthetic apparatus¹, in the oxidation of organic substrates* by cytochrome P450, and in the reduction of oxoanions³ such as nitrite and sulfite in bacteria, has prompted extensive investigations of various aspects of metalloporphyrin chemistry. The use of photochemistry to induce such reactivity is an approach of much current activity. It is therefore appropriate to bring together the various photochemical studies of first row transition metalloporphyrins. The complexes of chromium, manganese, and iron have been by far the most carefully examined. Consequently, we will limit our review to complexes of these metals.

The absorption spectra of metalloporphyrins are diverse and complex. Any discussion of porphyrin photochemistry profits from an understanding of the electronic transitions responsible for the observed spectra. As such, the first section of this review contains an overview of the observed types of spectra. We then describe a general categorization of metalloporphyrin photochemistry. This classification scheme provides a good framework for the discussion of the photochemistry of first row transition metal porphyrins. The last section of the review focuses in turn on the photochemistry of chromium, manganese, and iron porphyrin complexes.

Metalloporphyrin electronic spectra

As shown in Figure 1, there are three classes of metalloporphyrin electronic spectra. These have been called normal, hypso,

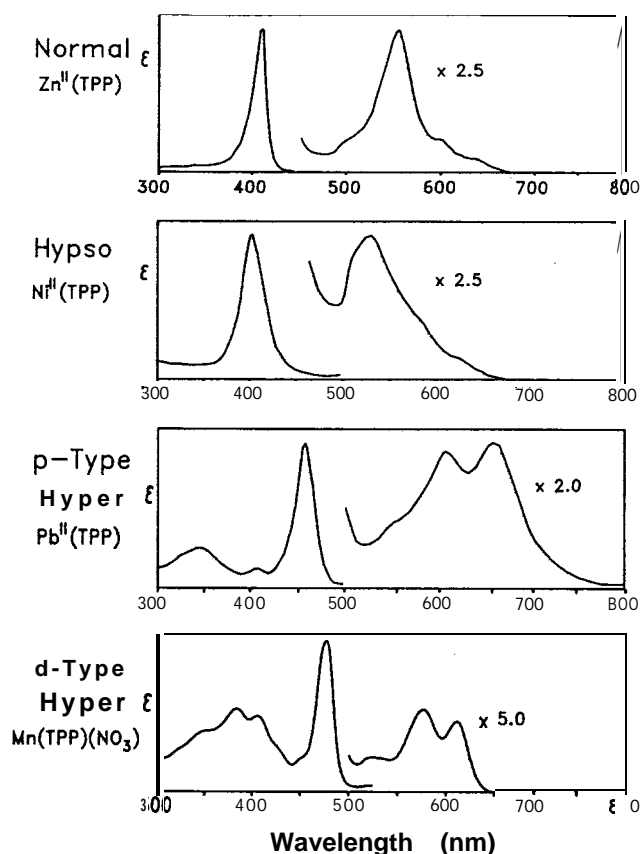


Figure 1. — Representative electronic spectra of metalloporphyrins from each of the four classes discussed in the text.

and hyper, with the hyper spectra being further divided into P-type and d-type. This is the classification scheme of Gouterman⁴ and will be used throughout this review. Our discussion of these classes will be qualitative; detailed analyses have been presented elsewhere⁴. While there is agreement on the general types of transitions involved, the exact nature of ground and excited state electronic configurations continue to be explored⁵.

NORMAL SPECTRA

Normal spectra are observed for metalloporphyrins with metals from groups 1 to 5 with oxidation states of I to V, respectively, and for other d^0 or d^{10} metals. Characteristically, **normal** spectra have one intense absorbance (the Soret or B-band) between 320 and 450 nm and one or two absorbances (Q bands) between 450 and 700 nm. Meso-substituted porphyrins often show a merging of the lower energy bands. Metal-free porphyrins also have **normal** spectra, although they have a four-banded spectrum between 450 and 700 nm. This increase in the number of bands is attributed to lowering of the D_{4h} symmetry of the metalloporphyrin to D_{2h} by protonation of two pyrrole nitrogens in the metal-free porphyrin.

Normal spectra are well explained by Gouterman's four-orbital model⁴. In this model, the four orbitals are porphyrin π and π^* orbitals; the two highest occupied molecular orbitals (HOMO's) of a_1 and a_{2u} symmetry, and the two lowest unoccupied molecular orbitals (LUMO's) of e_g symmetry (Fig. 2). The two major absorbances arise from coupling of the two transitions between the HOMO's and LUMO's ($\pi \rightarrow \pi^*$) (Fig. 3). The Q bands are the result of the transition dipoles nearly canceling each other out, therefore resulting in a weaker absorbance. The higher energy Soret transition results from a linear combination of the two transitions with reinforcing transition

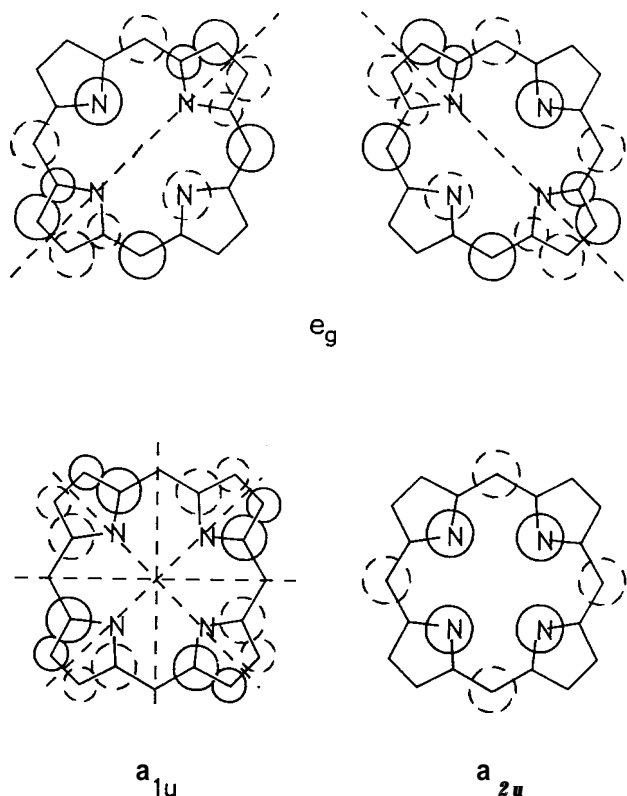


Figure 2. - The highest occupied molecular orbitals (a_1 and a_{2u} symmetry) and the lowest unoccupied molecular orbital (e_g symmetry) of metalloporphyrins (adapted from reference 4).

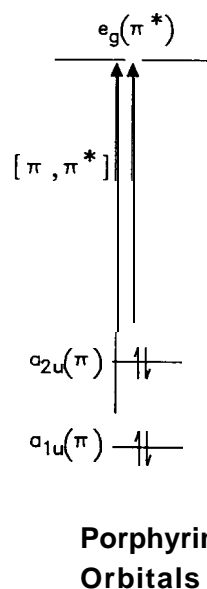


Figure 3. - Molecular orbital diagram for the four-orbital model of normal metalloporphyrin absorbances.

dipoles and is therefore very intense. Some shifts in the positions of the bands as a function of metal occur due to weak interaction of the metal with the a_{2u} and e_g orbitals. As shown in Figure 2, the a_1 orbital has nodes at the pyrrole nitrogens and therefore remains relatively unaffected by the metal⁶. Because the transitions are largely porphyrin-ring based, little photochemistry is expected to occur in complexes with **normal** spectra; this is borne out by experimental observations.

HYPSO SPECTRA

The **hypso** porphyrins have spectra which look very much like the **normal** porphyrins except that the Q-band is blue shifted to wavelengths of less than 570 nm as shown in Figure 1. The hypso spectrum is found with transition metal complexes with electron counts of d^6 to d^9 and therefore filled $e_g(d_\pi)$ orbitals⁷. Common examples are Pd^{II} , Pt^{II} , Rh^{II} , and Ni^{II} . The blue shift in the Q-band is explained by mixing of the e_g LUMO of the porphyrin ring with the filled $e_g(d_\pi)$ metal orbitals. This interaction pushes the porphyrin LUMO to higher energy as shown in Figure 4, thus increasing the $\pi-\pi^*$ energy gap of the porphyrin. The overlap is greatest for **4d** and **5d** metals, which show the largest blue-shifts. Within a given row of transition metals, the energy of the d_π electrons decreases with increasing electron count. Thus, as the number of d-electrons increase, the energy gap between the porphyrin LUMO and the metal increases, and the orbital mixing decreases. For the late first-row transition metal ions, the spectra become less blue shifted as the d-electron count increases from Fe^{II} , Co^{II} , Ni^{II} , Cu^{II} , to Zn^{II} . As pointed out by Gouterman⁴, Zn^{II} porphyrins actually have normal spectra. Of the hypso porphyrins, Fe^{II} is perhaps one of the more interesting cases. The Fe^{II} porphyrins may exhibit either hypso (if $S=0$) or hyper (if $S>0$, discussed below) spectra.

HYPHER SPECTRA

The **hyper** spectra, both **p-type** and **d-type**, show additional absorbance compared to the normal and **hypso** varieties. These additional bands are generally to the blue of the Q-band and are of moderate intensity, as shown in Figure 1. Main group elements in low oxidation state (e.g., Sn^{II} , Pb^{II} , P^{III} , As^{III}) give

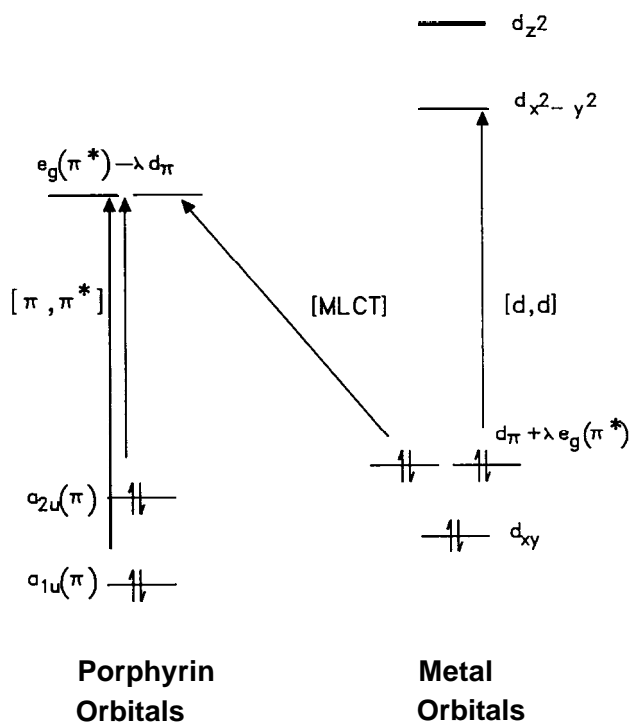


Figure 4. Molecular orbital diagram for *hypso* metalloporphyrins (adapted from reference 7).

p-type *hyper* spectra. In this case the extra bands are due to metal to ligand charge transfer⁸⁻¹⁰. As shown in Figure 5, the charge transfer originates in the metal p_z orbital and is $a_{2u}(np_z)(\text{metal}) \rightarrow e_g(\pi^*)$ (ring).

Of more interest to this review are the porphyrin complexes that exhibit d-type *hyper* spectra. This type of spectrum is found with d^1 through d^6 metals that have vacancies in the $e_g(d_\pi)$ orbitals⁴. These vacancies make a porphyrin ligand-to-metal charge transfer transition possible, as shown in Figure 6.

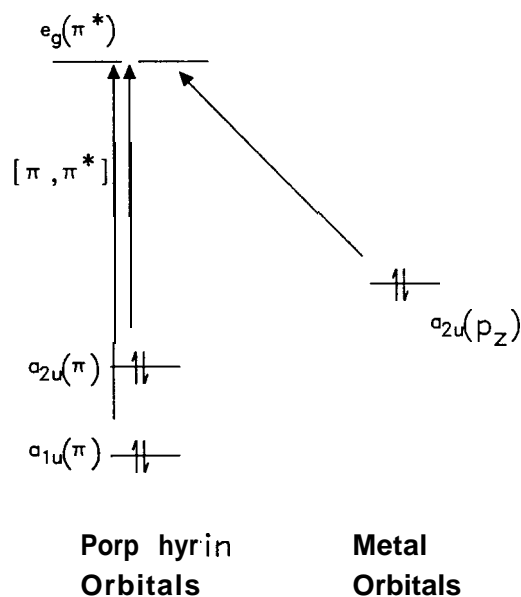


Figure 5. - Molecular orbital diagram for p-type *hyper* metalloporphyrins (adapted from reference 4).

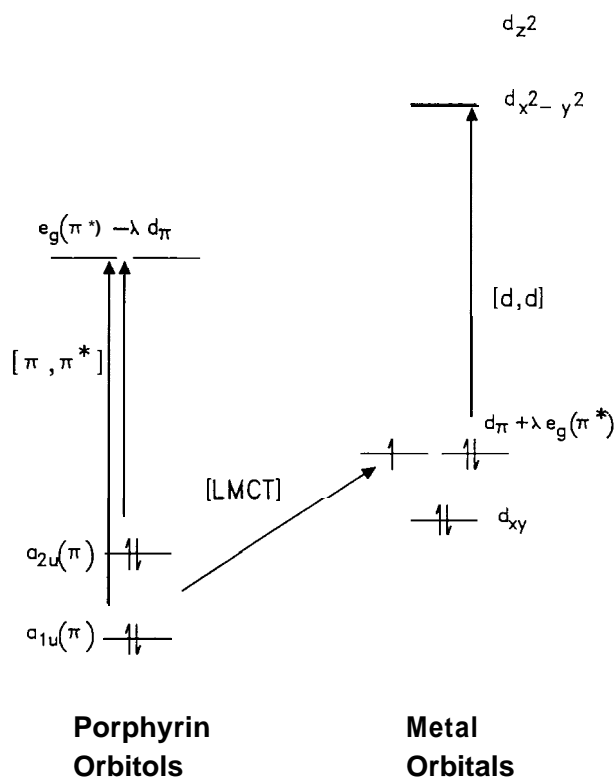


Figure 6. - Molecular orbital diagram for d-type *hyper* metalloporphyrins (adapted from reference 8).

Because the charge transfer results in a change of metal oxidation state, relatively low metal redox potentials are also desirable to make the final product more stable¹¹. There is also considerable mixing of the metal d_π orbitals with the LUMO of the porphyrin, since they are of the same symmetry (e_g)¹². The extensive mixing then accounts for the complex spectra often observed in d-type *hyper* porphyrins. This mixing occurs more readily when the porphyrin LUMO is close in energy to the metal orbitals. Calculations have shown¹¹ that Cr^{III} , Mn^{III} , and Fe^{II} metal orbitals are uniquely situated in energy for extensive mixing to occur. It is this extensive mixing of metal and porphyrin orbitals that makes, Cr, Mn, and Fe porphyrins of greatest interest for photochemical studies. As will be seen throughout the next section, a variety of photochemical processes occur with metalloporphyrins having d-type *hyper* spectra.

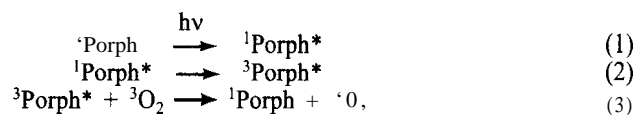
General classes of porphyrin photochemistry

There are a variety of classification schemes into which porphyrin photochemistry might be divided, depending on the aspects one wishes to emphasize. For our purposes, three classes will be used: photosensitization, photoreduction of the metal, and photooxidation of the metal.

PHOTOSENSITIZATION

In photosensitization reactions, the porphyrin undergoes no permanent changes. There are a variety of processes wherein the porphyrin acts as an absorber and energy transfer agent (i.e., a sensitizer), and much effort has been made in the area. Perhaps the most important and well known example is the singlet-singlet energy transfer that forms the primary steps of light-energy harvesting in photosynthesis by so-called antennae chlorophylls¹³.

Another example of growing importance is the use of porphyrins in photodynamic therapy (PDT) for cancer treatment¹⁴⁻¹⁶. It is well known that porphyrins and metalloporphyrins have a small energy gap between the lowest singlet and triplet states and that the intersystem crossing can be very efficient¹⁷. Thus, after excitation to an excited singlet state, the triplet is formed in high yields (Eq. 1 and 2). This energy may then be transferred to ground state triplet oxygen to produce the highly reactive singlet oxygen ($^1\Delta_g$), as shown in Equation 3.



The singlet oxygen thus produced may then oxidize organic substrates. In the case of PDT, this results in the destruction of tumor tissue in which the porphyrin sensitizer has preferentially accumulated. Alternatively, the triplet state of the porphyrin may abstract hydrogen from nearby substrate and initiate a variety of radical reactions that also may ultimately destroy the tumor. In either case, the porphyrin is generally left unchanged at the end of the cycle. Secondary decomposition of the porphyrin due to $^1\text{O}_2$ reactions or to metabolism of the porphyrin itself will eventually occur in vivo.

PHOTOREDUCTION AND PHOTOOXIDATION

Excited states formed on irradiation are well known to be both better reductants and better oxidants than the ground state molecule. Because of this, both reductions and oxidations are common photochemical reactions. The reduction or oxidation of porphyrins on irradiation can occur either on the ring or at the metal center (if the porphyrin is metallated). Examples of reactions of the porphyrin ring or its substituents are diverse.

The photooxidation of porphyrinogens (which are porphyrinic macrocycles with four reduced methine carbons) to porphyrins is known to occur in the presence of oxygen¹⁸. Similarly, metallochlorins (a metalloporphyrin with one pyrrole reduced) may be photooxidized to metalloporphyrins. The oxidation of unsaturated side chains in porphyrins such as protoporphyrin IX in organic solvents has also been reported¹⁷. In all of these photooxidations, the presence of oxygen is important, possibly due to formation of singlet molecular oxygen as discussed above.

The photoreductions of both porphyrins and metalloporphyrins are also known. In these cases reducing agents such as ascorbic acid, glutathione, EDTA, or ethyl acetoacetate are necessary¹⁷. In strongly acidic solutions, porphyrins can be rapidly photoreduced to chlorins and bacteriochlorins. These reductions are often thermally reversible. Metalloporphyrins undergo analogous photoreductions. For both porphyrins and metalloporphyrins, phlorins (where the site of reduction is a methine carbon) are the initial photoproducts. The chlorins are then formed by a rapid rearrangement.

Photo-redox reactions involving the metal center are potentially more diverse. Recently, several such reactions have been observed and are discussed in depth in the next section of this review. In general terms, it can be said that for a redox reaction to occur there must be a second stable oxidation state available to the metal. This explains why the majority of known photo-redox processes involve group 5 to 7 metals. As will be seen in the next section, solvent and cage effects can also play critical roles, although the mechanism of such effects are not always clear.

Photochemistry of chromium porphyrins

There has been relatively little photochemical research with chromium porphyrins. This may be due to emphasis on the more biologically relevant iron complexes. The work that has been done has centered around two areas: photochemically assisted oxygen atom transfer and photooxidation of chromium azido complexes.

It has been reported^{19,20}, that the formation of $\text{Cr}^{\text{V}}(\text{TPP})(\text{O})$ (Cl) from $\text{Cr}^{\text{III}}(\text{TPP})(\text{Cl})$ and *p*-cyano-N,N-dimethylaniline N-oxide occurs only during irradiation. The high valent species was shown to then quantitatively oxidize 1-phenyl-1,2-ethanediol. The same reaction occurs thermally with manganese and iron porphyrins. There is some question as to whether the observed photochemistry is a result of light absorption by the porphyrin or by N-oxide. Whichever the case, the apparent quantum yield is very high since fluorescent room lights are sufficient to drive the reaction.

In a similar vein, the transfer of an oxygen atom from coordinated perchlorate to the metal has been reported²¹ for $\text{Cr}^{\text{III}}(\text{TPP})(\text{ClO}_4)$ forming $\text{Cr}^{\text{IV}}(\text{TPP})(\text{O})$. In this case, the reaction observed on irradiation depends on the solvent used and substrate present. In solvents which are relatively difficult to oxidize, such as toluene and benzene, $\text{Cr}(\text{TPP})(\text{ClO}_4)$ was observed on irradiation to first yield $\text{Cr}^{\text{IV}}(\text{TPP})(\text{O})$ with good isosbestic behavior. This occurred with a quantum yield of 1.3×10^{-4} . This species was then converted to $\text{Cr}^{\text{III}}(\text{TPP})(\text{Cl})$ quantitatively. In more easily oxidized solvents, such as cyclohexene, the photoreaction went directly to $\text{Cr}^{\text{III}}(\text{TPP})(\text{Cl})$, with little $\text{Cr}^{\text{IV}}(\text{TPP})(\text{O})$ observed. In both reactions, the oxidation of substrate was observed. In toluene, 0.75 equivalents of benzaldehyde were produced, representing 1.50 oxidation equivalents. In cyclohexene, a mixture of products (cyclohexene oxide, cyclohexenol, cyclohexenone, and 1,2-cyclohexanedione) totaling 1.86 oxidation equivalents was observed.

It was proposed in this work²¹ that the oxidation products were due to radical based ClO_x species and not to porphyrin metal-oxo species. The $\text{Cr}^{\text{IV}}(\text{TPP})(\text{O})$ is known²² to be incapable of the types of oxidations observed, and in the same work it was shown that it could not be photochemically activated to do such oxidations. The intermediacy of $\text{Cr}^{\text{IV}}(\text{TPP})(\text{O})$ was observed in cases where the radical based oxidations were difficult. This slows the production of Cl which is responsible for $\text{Cr}(\text{TPP})(\text{Cl})$ formation. In easily oxidized solvents, the Cl[•] is produced so rapidly that formation of $\text{Cr}(\text{TPP})(\text{Cl})$ is directly observed.

The second example of chromium photooxidation involves the photochemical transformation of $\text{Cr}^{\text{III}}(\text{porph})(\text{N}_3)$ to $\text{Cr}^{\text{V}}(\text{porph})(\text{N})$ and dinitrogen^{23,24}. This reaction has been shown to be quantitative for a variety of porphyrins (e.g., 5,10,15,20-tetratolylporphyrin, 5,10,15,20-tetraphenylporphyrin, 5,10,15,20-tetramesitylporphyrin) and appears to be unaffected by changes of the porphyrin substituents. The nitrido species formed is very stable, and no nitrogen atom transfer to substrates is observed.

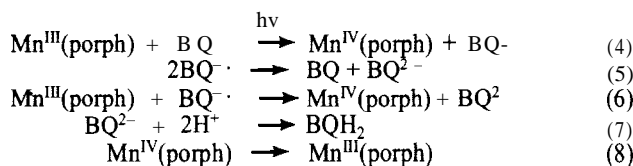
Photochemistry of manganese porphyrins

There has been a great deal of interest over the last decade in the photochemistry of manganese porphyrins, for a variety of reasons, including their unique electronic properties, their robustness as oxidation catalysts, and their potential relevance to photosynthetic processes¹. The research spans a rather wide area, including the use of manganese porphyrins as photosensitizers in conjunction with other molecules for electron transfer

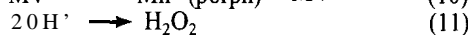
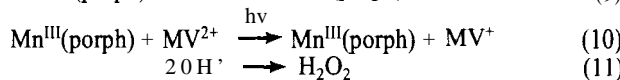
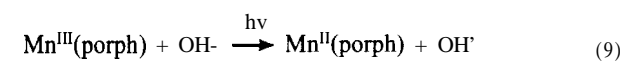
(an area not covered in this review)^{25,26}, and the use of photochemically generated species for substrate alteration (e.g., epoxidation, hydroxylation, azidification).

The extensive work of Harriman et al.²⁷⁻²⁹ on the photochemistry of water-soluble manganese porphyrins was an early attempt to construct an in vitro model system for the photooxidation of water. In an early study²⁷ it was shown that $Mn^{III}(TPyP)$ (where TPyP is 5,10,15,20-tetra(4-pyridyl)porphyrin), on irradiation in ethanol produced $Mn^{II}(TPyP)$ and acetaldehyde with a quantum yield of 1.2×10^{-4} . On re-exposure to air, more than 95% $Mn^{III}(TPyP)$ was regenerated. The quantum yield was shown to be independent of the water solubilizing groups on the porphyrin ring. A pH dependence was noted; at higher pH, the quantum yield increased due to increased OH⁻ availability for electron donation. It was noted that no decomposition of $Mn^{II}(TPyP)$ occurred on irradiation in the absence of good hydrogen donors. In the presence of ascorbic acid, however, photoreduction of the porphyrin ring gave hydroporphyrins.

In other studies, the reduction of benzoquinone²⁸ and methylviologen²⁹ by irradiation of various water soluble manganese porphyrins was reported. Irradiation in the presence of benzoquinone (BQ) produces no observable changes in the absorption spectrum of the porphyrin, except for a small amount of bleaching. The quantum yield of BQH₂ formation and the extent of porphyrin bleaching has been studied under a variety of conditions. Typically the quantum yields were ≈ 0.05 , and after 5 turnovers, less than 10% bleaching occurred. Harriman proposed an unusual photooxidation of the manganese porphyrin as the first step of his mechanism (Eq. 4), although the manganese(IV) species was never observed. Through a series of subsequent steps (Eq. 5-8) BQH₂ is formed. The $Mn^{III}(\text{porph})$ is eventually regenerated via thermal reduction by water and buffer (Eq. 8).

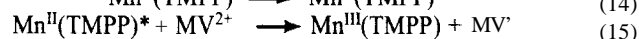
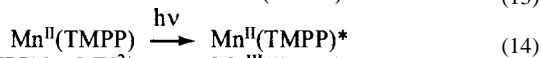
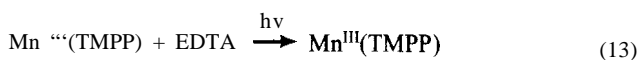


A similar reduction of methylviologen (MV^{2+}) occurs upon irradiation in strongly alkaline solutions. In this reaction, however, photoreduction of the manganese porphyrin initially occurs, as shown in Equation 9. The $Mn^{II}(\text{porph})$ then reduces the MV^{2+} to MV^+ on continued irradiation, regenerating $Mn^{III}(\text{porph})$ (Eq. 10). On prolonged irradiation, a steady state concentration of MV^+ is produced and $Mn^{II}(\text{porph})$ is the predominate porphyrin species observed. Due to recombination of OH⁻ to give H₂O₂ the overall net reaction is given by Equation 12.



In similar work³⁰ in aqueous media, the photoreduction of $Mn^{III}(TMPP)$ (where TMPP is 5,10,15,20-tetrakis(4-methylpyridyl)porphyrin) was reported in the presence of electron donors such as EDTA, triethanolamine (TEOA), and triethylamine. By varying the strength and concentration of the electron donor in the presence of porphyrin and methylviologen, some interesting photochemistry resulted. In the presence of the strong electron donor EDTA, there was initially photoreduction

to $Mn^{II}(TMPP)$ (Eq. 13). This is followed by the eventual regeneration of $Mn^{III}(TMPP)$ and reduction of MV^{2+} to MV^+ via a $Mn^{II}(TMPP)$ excited state (Eq. 14 and 15). The reduction by excited state $Mn^{II}(TMPP)$ was proposed because the ground state of $Mn^{II}(TMPP)$ ($E_{1/2}^{III/II} = -0.21V$) is not a strong enough reductant to reduce MV^{2+} ($E^0 = -0.67V$). This is similar to the mechanism proposed in Harriman's work on water oxidation (Eq. 10). Using weak electron donors such as TEOA, a different mechanism was invoked by Takahashi et al., who proposed that excited state $Mn^{III}(TMPP)^*$ was oxidized by MV^{2+} . This requires the energy level of the excited state to be approximately 1.12 eV above the ground state.



The photoreduction of manganese porphyrins has also been well established in non-aqueous media. Imamura et al. have examined a number of manganese(III) halides and other simple ligands at room temperature³¹ and in frozen glasses³². As shown in Table I, the quantum yields of the photoreduction in 2-methyltetrahydrofuran (MeTHF) are of same order of magnitude as those processes already discussed. Interestingly, in MeTHF glasses at 77K, no photoactivity was observed for any of the compounds listed in Table II. No explanation for this observation was volunteered by the authors.

Table I. - The photoreduction of manganese porphyrins*.

| Mn ^{III} (TPP)X | hν | Mn ^{II} (TPP) + X [·] |
|--------------------------|----|---|
| X | | φ |
| I | | 1 × 10 ⁻⁴ |
| Br | | 3 × 10 ⁻⁷ |
| Cl | | 2 × 10 ⁻⁶ |
| OAc | | 1 × 10 ⁻⁷ |
| NCS | | 2 × 10 ⁻⁴ |

* From reference 28; solvent was MeTHF.

Three separate groups have examined^{24,32-34} the photochemistry of $Mn^{III}(\text{porph})(N_3)$. In reactions similar to those of chromium azide complex discussed earlier, $Mn^{III}(\text{porph})(N_3)$ forms $Mn^V(\text{porph})(N)$ quantitatively on photolysis in benzene³³ or toluene²⁴. The nitrido species thus formed is quite stable and may be isolated by chromatography. Derivatization with trifluoroacetic anhydride to an acylimidomanganese(V) species allows transfer of the acylimido group to unsaturated molecules in what is called the azo-analogue to epoxidation³³.

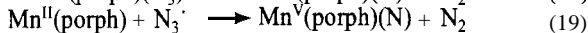
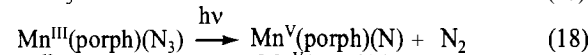
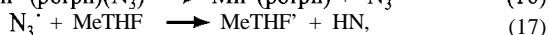
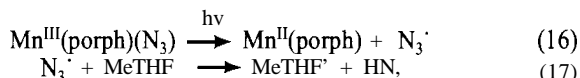
Interestingly, photoreduction of $Mn^{III}(\text{porph})(N_3)$ to $Mn^{II}(\text{porph})$ is observed at room temperature in MeTHF^{32,34} instead of photooxidation to $Mn^V(\text{porph})(N)$. At temperatures of less than -80° C, however, in the same solvent the photooxidation is again observed. At intermediate temperatures, both $Mn^{II}(\text{porph})$ and $Mn^V(\text{porph})(N)$ are formed together. Spin trapping experiments at room temperature suggest the formation of MeTHF[·] radicals. It was thus proposed that in first step of the room temperature photoreaction $Mn^{II}(\text{porph})$ and $N_3^·$ are formed as in Equation 16. The $N_3^·$ radical formed is then quickly scavenged by solvent to give MeTHF[·] and HN_3 (Eq. 17). This process is not observed in benzene or toluene, consistent with the less easily abstracted hydrogens of these

Table II. - Photocatalytic oxidation of hydrocarbons by Mn(TPP)(X)*.

| Mn complex | Oxoanion ^a | Substrate | Product(s) | Equivalents per Mn |
|----------------------------|-------------------------------|---|---|--------------------|
| Mn(TPP)(ClO ₄) | ClO ₄ ⁻ |  |  | 1.94 |
| Mn(TPP)(ClO ₄) | ClO ₄ ⁻ |  |  | 1.78 |
| | | |  | 0.30 |
| | | |  | 0.66 |
| Mn(TPP)(ClO ₄) | ClO ₄ ⁻ |  |  | 1.67 |
| Mn(TPP)(OAc) | IO ₄ ⁻ |  |  | 2.40 |
| Mn(TPP)(OAc) | IO ₄ ⁻ |  |  | 11.3 |
| | | |  | 3.30 |
| | | |  | 1.04 |
| Mn(TPP)(OAc) | IO ₄ ⁻ |  |  | 6.00 |

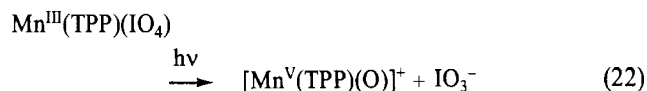
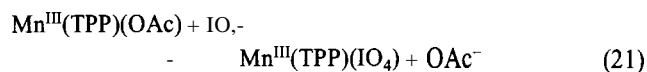
^a Reactions with ClO₄⁻ are stoichiometric while those using IO₄⁻ are catalytic; * From reference Ha.

solvents. Imamura and coworkers proposed a competing photochemical process (Eq. 18) to explain the low temperature photooxidation.



This mechanism, however, overlooks the additional possibility of a thermal reaction (Eq. 19) with N₃[·] to give Mn^V(porph)(N) and N₂. This would be favored under conditions of long N₃[·] lifetime, including photolysis in solvents that cannot be reduced or at low temperatures where solvent reduction is slowed. This possibility is also consistent with the reported observations and has been confirmed in analogous iron systems (*vide infra*).

In more recent work^{21,35} it has been reported that irradiation of Mn^{III}(TPP)(ClO₄) quantitatively forms Mn^{III}(TPP)(Cl) with a quantum yield of 2.7 x 10⁻⁵ (Eq. 20). In this work, it was discovered that substrate oxidation of hydrocarbons incorporated all four oxygen equivalents of the oxoanion (Table II). With IO₄⁻ as axial ligand the reaction was made catalytic by adding excess IO₄⁻ as the tetra n-hexylammonium salt (Eq. 21-23). This does not work with ClO₄⁻ because the Cl⁻ produced binds the manganese porphyrin too tightly to be replaced by excess Oxoanion. Based on the comparison of the observed oxidation chemistry and the known thermal chemistry of porphyrin metal-oxo species, [Mn^V(TPP)(O)]⁺ was proposed as the active oxidant in the system. Such a species is too reactive to be observed directly at room temperature²².



In an extension of this work, the photochemistry of other manganese porphyrin oxoanion complexes has been examined with interesting results. It has been shown³⁶ that on irradiation between 350 and 420 nm, both Mn(TPP)(NO₃) and Mn(TPP)(NO₂) undergo a two-step process resulting finally in Mn^{II}(TPP). In the first step, the complexes are converted to Mn^{IV}(TPP)(O) with a quantum yield of 1.6 x 10⁻⁴ for the nitrate and 5.3 x 10⁻⁴ for the nitrite complex. Mn^{II}(TPP) is formed quantitatively in both cases on reaction of Mn^{IV}(TPP)(O) with oxidizable substrate. It was shown in reactions with styrene and triphenylphosphine that in the case of the nitrate complex, two oxidizing equivalents per Mn(TPP)(NO₃) were available. For Mn(TPP)(NO₂) on the other hand, only one oxidation equivalent was realized. Based on these results and other confirmatory experiments, it was proposed that Mn(TPP)(NO₂) is formed during the photolysis of Mn(TPP)(NO₃) and is responsible for the second oxidizing equivalent (Fig. 7).

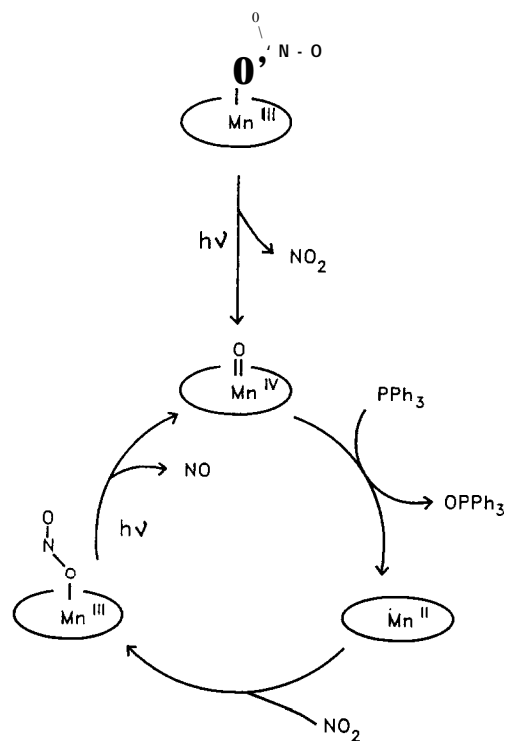
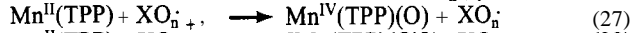
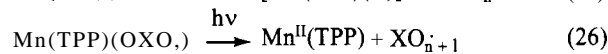
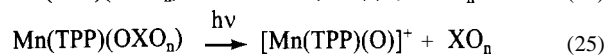
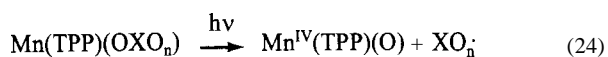


Figure 7. - Photochemical reaction cycle of Mn porphyrin nitrate and nitrite complexes (reference 36).

In contrast to the manganese ClO₄⁻, NO₃⁻, and NO₂⁻ complexes, the SO₄²⁻ and HSO₄⁻ complexes do not form metal-oxo species on irradiation, and no oxidation of hydrocarbons is observed. Instead, both [Mn(TPP)]₂(SO₄) and Mn(TPP)

(OSO₃H) directly form Mn^{II}(TPP) with quantum yields of 7.0×10^{-4} and 9.8×10^{-4} respectively³⁷. In both cases, the formation of 1.0 equivalents of OP(C₆H₅)₃ was observed if the photolysis was carried out in the presence of P(C₆H₅)₃, though this oxidation did not directly involve the porphyrin. The ultimate fate of the axial ligands has not been determined; production of either SO₂ and O₂, however, are not observed.

In my work with manganese porphyrin oxoanion complexes, two distinct types of reactivity are observed: oxygen atom transfer to the metal and photoreduction of the metal. In the first class, both nitrate and nitrite complexes underwent P-bond cleavage to form Mn^{IV}(TPP)(O) (Eq. 24). In the case of perchlorate and periodate complexes, the formation of [Mn(TPP)(O)]⁺ was inferred from the nature of the observed hydrocarbon oxidations (Eq. 25). On the other hand, sulfate and bisulfate complexes underwent homolytic a-bond cleavage to form Mn^{II}(TPP), as shown in Equation 26. The possibility that all oxoanion complexes may actually undergo initial a-bond cleavage as in Equation 26, followed in some cases by a rapid thermal reaction to form metal-oxo species (Eq. 27-28), was also recognized. Solution photochemical studies could not differentiate between these two mechanisms.



Experiments using matrix isolation techniques can prevent, in principal, the thermal reactions shown in Equations 27 and 28; it was shown³⁸ that all of the manganese porphyrin oxoanion complexes actually undergo the same primary photochemical reaction: photoreduction. In reactions carried out in low temperature (10K) polymer films and solvent glasses, no metal-oxo formation was observed. This observation, together with all of the other manganese porphyrin photochemistry discussed here, suggests that initial photoreduction of the metal center is a general reaction of all manganese porphyrins. The subsequent thermal chemistry is probably determined by several factors, including the relative stabilities of the leaving groups and the remnant porphyrin species, as well as relative solvation energies of products.

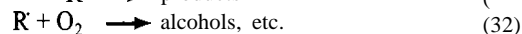
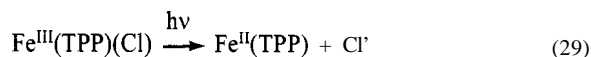
Photochemistry of iron porphyrins

There are two major research areas that involve the photochemistry of iron porphyrins. The first of these is the flash photolysis examination of ligand-rebinding processes, primarily CO rebinding to iron(II) porphyrins and heme proteins. While there have been many interesting findings and new techniques developed in this work, a review of the vast literature of this area is beyond the scope of this review^{39, 40}. The second major area involves photoredox chemistry similar to that of chromium and manganese porphyrins.

A review of the iron porphyrin literature reveals very few examples of photooxidation of the iron center. In many of these cases, which were believed at first to be photooxidations, later studies revealed them to be initial photoreductions followed by rapid thermal reactions resulting in oxidation of the metal center. As will be seen, there is still an interesting variety of chemistry that can result from such secondary reactions. A notable

result is the observation by Nakamoto⁴¹ that laser photolysis of the co-condensation products of Fe(porph) with O₂ at 15 K unexpectedly produced Fe^{IV}(porph)(O).

The photoreduction of Fe^{III}(porph)(X) where X is a halide or hydroxide has been well established^{31, 42}. By examining the energy of absorbance bands as a function of axial ligation, Suslick et al.⁴² have assigned the near-UV absorption that is responsible for this photoreduction as a halide-to-metal charge transfer. In the same work it was also shown that the rate of photoreduction was highly dependent upon the solvent: quantum yields decreased from cumene > ethylbenzene > toluene > cyclohexane. A clear linear free-energy relationship between the reduction rate and the bond dissociation energy of the solvents was shown. Most interestingly they demonstrated that if the irradiation is carried out in the presence of oxygen the photoinitiation of substrate oxidation occurs as per Equations 29-32. Thus on photolysis in cyclohexene, over 150 equivalents of allylic oxidation products are formed for each porphyrin equivalent. Similarly in cumene 160 equivalents of oxidation products are formed. The quantum yields of these oxidations are 0.26 in cyclohexene and 0.30 in cumene. The final porphyrin product is [Fe(TPP)]₂(O).



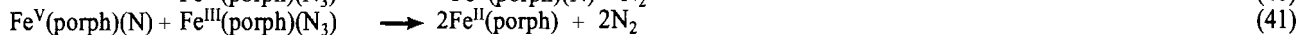
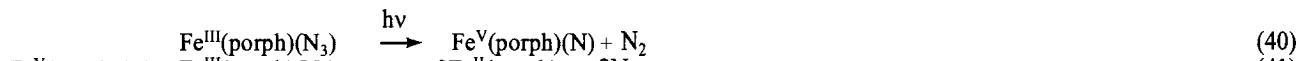
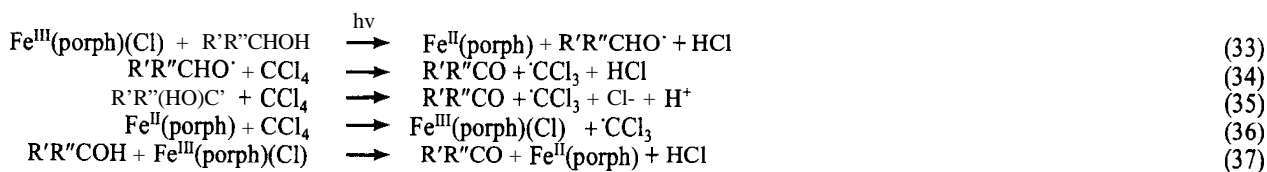
The photoreduction of iron(III) porphyrins in alcoholic solvents has been extensively studied by Carassiti and coworkers using both synthetic porphyrins⁴³⁻⁴⁸ and naturally occurring porphyrins⁴⁹⁻⁵¹. As shown in Table III, a variety of porphyrins and alcohols have been examined with similar results. In fact, in a detailed study⁴⁸ it was shown that there is no change in the photoreduction quantum yield as the electron donating or withdrawing strength of porphyrin ring substituents are changed. This is consistent with the proposal that an axial-ligand to metal charge transfer band is responsible for the observed photochemistry.

Table III. - Photoreduction of iron(III) porphyrin complexes.

| Complex | Solvent | #(reduction) | Reference |
|--|--|----------------------|-----------|
| Fe(TPP)(Cl) | MeTHF | 8×10^{-7} | 28 |
| Fe(TPP)(Cl) | benzene | 5.1×10^{-4} | 36 |
| Fe(DPDME)(OC ₃ H ₇) | benzene/propanol | 2×10^{-2} | 37 |
| Fe(TDCPP)(OEt) | ethanol | 2×10^{-2} | 40 |
| Fe(TDCPP)(OiPr) | isopropanol | 4.5×10^{-2} | 40 |
| Fe(TPFPP)(OEt) | ethanol | 1.6×10^{-2} | 42 |
| Fe(TMP)(OEt) | ethanol | 1.9×10^{-2} | 42 |
| [Fe(TPP)] ₂ (O) | benzene/P(C ₆ H ₅) ₃ | 2×10^{-4} | 49 |
| [Fe(TPPC)] ₂ (O) | H ₂ O/TEOA | 5.2×10^{-5} | 48 |

DPDME = deuteroporphyrin dimethyl ester; TPFPP = 5,10,15,20-tetra(pentafluorophenyl)porphyrin; TMP = 5,10,15,20-tetra(p-tolyl)porphyrin; TDCPP = 5,10,15,20-tetra(2,6-dichlorophenyl)porphyrin; TPPC = 5,10,15,20-tetra(4-carboxyphenyl)porphyrin.

In each case, along with photoreduction of the metal, an alkoxide radical is also formed (Eq. 33). In the presence of CCl₄, a series of radical chain propagation steps are proposed that produce either aldehydes or ketones, depending on the alcohol used, coupled with the reduction of CCl₄ to CHCl₃ (Eq. 34 and 35). CCl₄ may also be reduced by Fe^{II}(porph), thus regenerating Fe^{III}(porph)(Cl) (Eq. 36). The net overall reaction then is given by Equation 38. The seemingly high quantum yields for these processes (Table III) are easily explained by Equation 37.

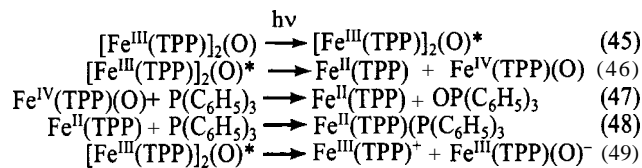


For each photon absorbed, many molecules of $\text{Fe}^{\text{II}}(\text{porph})$ can be formed. Porphyrin turnovers of greater than 130,000 have been reported in the photoreduction of CCl_4 .⁴⁶ In oxygenated aqueous ethanol, the formation of superoxide is observed, probably via Equation 39, where the ethanol radical is first formed following photoreduction of the porphyrin.

It has also been shown^{52, 53} that the $\text{Fe}^{\text{II}}(\text{porph})$ formed in the above mentioned photoreactions can be trapped by the addition of an appropriate ligand. Thus in ethanol solutions with added pyrazine (**pyz**) the formation of $\text{Fe}^{\text{II}}(\text{porph})(\text{pyz})_2$ is observed on irradiation. At low pyrazine concentrations, a polymeric species $[\text{Fe}^{\text{II}}(\text{porph})(\text{pyz})]_n$ is formed.

As with the chromium and manganese porphyrin azide complexes already discussed, $\text{Fe}^{\text{III}}(\text{porph})(\text{N}_3)$ is also photoactive²⁴ and forms $\text{Fe}^{\text{V}}(\text{porph})(\text{N})$. The iron species, however, is not as stable as the chromium and manganese analogs and the final product is the mixed valence species $\text{Fe}^{\text{IV}}(\text{porph})\text{-N-Fe}^{\text{III}}(\text{porph})$. Buchler proposed Equations 40-42 to explain this product. More recent work by Rehorek⁵⁴, has revealed an alternative mechanism to the direct photooxidation. Photolysis in the presence of a spin-trap such as N-tertbutyl-a-nitron or 3-nitrosodurene confirmed the formation of N_3^\cdot . This shows that, at least for some of the azido complex, the initial photoreaction is photoreduction to $\text{Fe}^{\text{II}}(\text{porph})$ and N_3^\cdot ; thermal reactions are subsequently responsible for the formation of the nitrido complex (Eq. 43 and 44).

Another iron porphyrin complex that displays interesting photochemistry is $[\text{Fe}^{\text{III}}(\text{porph})]_2(\text{O})$. Most of the work has been done with tetraphenylporphyrin in organic solvents⁵⁵⁻⁵⁷, although at least one water soluble porphyrin has also been used with the same results⁵⁸. In neat benzene, the complex appears to be photostable. On addition of $\text{P}(\text{C}_6\text{H}_5)_3$, the formation of $\text{Fe}^{\text{II}}(\text{TPP})(\text{P}(\text{C}_6\text{H}_5)_3)$ along with $\text{OP}(\text{C}_6\text{H}_5)_3$ is observed. The measured quantum yield for this process was 2×10^{-4} . The rate of production of $\text{Fe}^{\text{II}}(\text{TPP})$ was measured to be twice the rate of $\mu\text{-oxo}$ disappearance and twice the rate of $\text{OP}(\text{C}_6\text{H}_5)_3$ formation. This is all in keeping with the mechanism shown in Equations 45-48. Interestingly, if the irradiation is carried out in the presence of oxygen, the catalytic oxidation of simple olefins with over 1000 turnovers was observed yielding primarily allylic oxidation products, presumably from radical autoxidation chains. The original papers^{55, 56} reported no observation of heterolytic cleavage. A more recent study using picosecond photolysis proposes that, in addition to homolytic cleavage (Eq. 46), there is at least some heterolytic cleavage (Eq. 49). The products of the heterolytic cleavage likely undergo recombination much faster than the homolytic products due to added coulombic attraction.



The iron analogs of the manganese porphyrin oxoanion complexes discussed above have also been examined³⁶. In the case of $\text{Fe}(\text{TPP})(\text{NO}_3)$, the direct formation of $\text{Fe}^{\text{II}}(\text{TPP})$ is observed on irradiation. The oxidation of substrates, including C-H hydroxylation, is observed. This oxidation suggests that $\text{O}=\text{Fe}^{\text{IV}}(\text{TPP})^+$ is being formed as the active oxidant, although due to its extreme reactivity²² it is not directly observed. Remarkably, in tests with substrates such as toluene, styrene, and triphenylphosphine, all three oxygen equivalents are available for substrate oxidation. This is in contrast to $\text{Mn}(\text{TPP})(\text{NO}_3)$ where only two equivalents are available. Matrix isolation studies³⁸ of $\text{Fe}(\text{TPP})(\text{NO}_3)$ have surprisingly found $\text{Fe}(\text{TPP})(\text{NO}_3)$ to be photostable in frozen matrix. Likewise, both solution and matrix isolation studies of $\text{Fe}(\text{TPP})(\text{ClO}_4)$ have found it to be photostable.

Conclusions

The exploration of the photochemistry of porphyrin complexes of the first row transition metals continues to be an active area. Particularly well examined are metalloporphyrin complexes of chromium, manganese, and iron. Their photochemistry has revealed a diverse set of reactions. Examples include oxygen and nitrogen atom transfers, photoreductions, photooxidations, photocatalysis, and radical chain initiations. Table IV summarizes this range of reactivity.

There is growing evidence that much of this diversity actually represents secondary thermal reactions. In many cases, the primary photoprocess is homolytic loss of an axial ligand, resulting in photoreduction of the metal and production of a reactive radical from the lost ligand. Subsequent fast thermal reactions can then lead to the formation of the wide range of reactivity observed. To be sure, photoreduction may not prove to be the exclusive primary event, but it does appear to be the most prevalent.

This observation is consistent with the nature of the excited states involved. Irradiation of the low energy $\pi \rightarrow \pi^*$ transitions does not produce photochemical reactions in these complexes. Metalloporphyrins are unusual in this way: the observed photochemistry does not come from the lowest available excited

Table IV. - Summary of solution photochemistry of metalloporphyrin complexes.

| Reactants | Observed products | Reference |
|--|--|-----------|
| Cr ^{III} (porph)(Cl) + N-oxide | Cr ^V (porph)(O)(Cl) | 19, 20 |
| Cr ^{III} (porph)(ClO ₄) | Cr ^{IV} (porph)(O) | 21 |
| Cr ^{IV} (porph)(O) | [Cr ^{III} (porph)] ₂ (O) | 21b |
| [Cr ^{III} (porph)] ₂ (O) | Cr ^{II} (porph) | 21b |
| Cr ^{III} (porph)(N ₃) | Cr ^V (porph)(N) | 23, 24 |
| Mn ^{III} (porph) + EtOH | Mn ^{II} (porph) + acetaldehyde | 27 |
| Mn ^{III} (porph) + 2OH ⁻ + 2MV ²⁺ | Mn ^{III} (porph) + 2MV ⁺ + H ₂ O ₂ | 29 |
| Mn ^{III} (porph) + EDTA | Mn ^{II} (porph) | 30 |
| Mn ^{III} (porph) + MV ²⁺ | Mn ^{IV} (porph) + MV ⁺ | 30 |
| Mn ^{III} (porph)(X) | Mn ^{II} (porph) | 31, 32 |
| Mn ^{III} (porph)(N ₃) + benzene | Mn ^V (porph)(N) | 24, 33 |
| Mn ^{III} (porph)(N ₃) + 2-MeTHF | Mn ^{II} (porph) | 32, 34 |
| Mn ^{III} (porph)(ClO ₄) | Mn ^{III} (porph)(Cl) | 21a, 35 |
| Mn ^{III} (porph)(NO ₃) | Mn ^{IV} (porph)(O) | 36 |
| Mn ^{III} (porph)(NO ₂) | Mn ^{IV} (porph)(O) | 36 |
| [Mn ^{III} (porph)] ₂ (SO ₄) | Mn ^{II} (porph) | 37 |
| Mn ^{III} (porph)(OSO ₃ H) | Mn ^{II} (porph) | 37 |
| Fe ^{III} (porph)(X) | Fe ^{II} (porph) | 31, 42 |
| Fe ^{III} (porph)(N ₃) | Fe ^{IV} (porph)-N-Fe ^{III} (porph) | 24 |
| Fe(porph)(O ₂) | Fe ^{IV} (porph)(O) | 41 |
| [Fe ^{III} (porph)] ₂ (O) | Fe ^{II} (porph) + Fe ^{IV} (porph)(O) | 55, 56 |
| Fe ^{III} (porph)(NO ₃) | Fe ^{II} (porph) | 36 |

state. Instead, the excited states that show photochemistry are those involved in charge transfer transitions, either from the axial ligand to the metal or from the porphyrin itself to the metal. Thus, the preponderance of metalloporphyrin photochemistry is observed in complexes with hyper spectra.

The diversity of observed metalloporphyrin photochemistry bodes well for the future of this area. Applications to photocatalytic reactions, particularly in the oxidation of organic substrates, is still in early stages of development. It is likely that substantial progress will continue to be made here. The use of metalloporphyrin photochemistry in solid matrices may also prove to be of some utility. Finally, the examination of intermediates created photochemically has proved tremendously important for the O₂ binding heme proteins, and may also find uses in other heme proteins, such as cytochrome P450 and the hydroperoxidases.

REFERENCES

- Sauer K., *Acc. Chem. Res.*, 1980, 13, 249.
- Ortiz de Montellano P. R., Ed., "Cytochrome P450", Plenum, N. Y., 1985.
- Cole J. A., Ferguson S. J., Eds., "The Nitrogen and Sulfur Cycles", Cambridge University Press, Cambridge, 1988.
- Gouterman M., The *Porphyryns*, Dolphin D., Ed., Vol. III, p. 1, Academic, N. Y., 1978.
- Edwards W. D., Weiner B., Zemer M. C., *J. Phys. Chem.*, 1988, 92, 6188.
- Wang R. M. Y., Hoffman B. M., *J. Amer. Chem. Soc.*, 1984, 106, 4235.
- Antipas A., Buchler J. W., Gouterman M., Smith P. D., *J. Amer. Chem. Soc.*, 1978, 100, 3015.
- Schaffer A. M., Gouterman M., *Theor. Chim. Acta*, 1970, 18, 1.
- Gouterman M., Schwartz F. P., Smith P. D., Dolphin D., *J. Chem. Phys.*, 1973, 59, 676.
- Hanson L. K., Eaton W. A., Sligar S. G., Gunsalus I. C., Gouterman M., Connell C. R., *J. Amer. Chem. Soc.*, 1976, 98, 2612.
- Gouterman M., Hanson K. H., Khalil G. E., Leenstra W. R., Buchler J. W., *J. Phys. Chem.*, 1975, 62, 2343.

- Kobayashi H., Yanagawa Y., Osada H., Minami S., Shimizu M., *Bull. Chem. Soc. Jpn.*, 1973, 46, 1471.
- Huber R., *Angew. Chem. Int. Ed. Engl.*, 1989, 28, 848.
- Gomer C. J., *Sem. in Hematology*, 1989, 26, 27.
- Andreoni A., Cubeddu R., Eds., "Porphyrins in Tumor Phototherapy", Plenum, New York, 1984.
- Van der Bergh H., *Chem. Brit.*, 1986, 22, 430.
- (a) Hopf F. R., Whitten D. G., "The Porphyrins", Vol. II, Dolphin D., Ed., Academic, New York, 1978, pp. 161-209; (b) Kitagawa T., *Photomed. Photobiol.*, 1987, 9, 15.
- Mauzerall D., Granick S., *J. Biol. Chem.*, 1958, 232, 1141.
- Yuan L. C., Bruice T. C., *J. Amer. Chem. Soc.*, 1985, 107, 512.
- Yuan L. C., Calderwood T. S., Bruice T. C., *J. Amer. Chem. Soc.*, 1985, 107, 8273.
- (a) Suslick K. S., Acholla F. V., Cook B. R., *J. Amer. Chem. Soc.*, 1987, 109, 2818; (b) Suslick K. S., Acholla F. A., Watson R. A., *Inorg. Chem.*, in press.
- Hill C. L., Ed., "Activation and Functionalization of Alkanes", Wiley, N. Y., 1989, pp. 243-279.
- Groves J. T., Takahashi T., Butler W. M., *Inorg. Chem.*, 1983, 22, 884.
- Buchler J. W., Dreher C., *Z. Naturforsch.*, 1984, 39b, 222.
- Nango M., Mizusawa A., Takenori M., Yoshinago J., *J. Amer. Chem. Soc.*, 1990, 112, 1640, and references therein.
- Nango M., Kryo H., Loach P. A., *J. Chem. Soc. Chem. Comm.*, 1988, 697, and references therein.
- Harriman A., Porter G., *J. Chem. Soc. Faraday II*, 1979, 75, 1543.
- Harriman A., Porter G., *J. Chem. Soc. Faraday II*, 1980, 76, 1429.
- Camieri N., Harriman A., *J. Photochem.*, 1981, 15, 341.
- Takahashi K., Komura T., Imanaga H., *Bull. Chem. Soc. Jpn.*, 1983, 56, 2303.
- Imamura T., Jin T., Suzuki T., Fujimoto M., *Chem. Lett.*, 1985, 847.
- Jin T., Suzuki T., Imamura T., Fujimoto M., *Inorg. Chem.*, 1987, 26, 1280.
- Groves J. T., Takahashi T., *J. Amer. Chem. Soc.*, 1983, 105, 2073.
- Imamura T., Yamamoto Y., Suzuki T., Fujimoto M., *Chem. Lett.*, 1987, 2185.
- Suslick K. S., Acholla F. V., Cook B. R., Kinnaird M. G., *Recl. Trav. Chim. Pays-Bas*, 1987, 106, 329.
- Suslick K. S., Watson R. A., *Inorg. Chem.*, 1991, 30, 912.

- ³⁷ Suslick K. S., Watson R. A., Wilson S. R., *Inorg. Chem.*, 1991, **30**, 2311.
- ³⁸ Suslick K. S., Bautista J. B., Watson R. A., *J. Amer. Chem. Soc.*, 1991, **113**, 6111.
- ³⁹ Miers J. B., Postlewaite J. C., Cowen B. R., Roemig G. R., Lee I. S., Dlott D. D., *J. Chem. Phys.*, 1991, 94, 1825, and references cited therein.
- ⁴⁸ (a) Frauenfelder H., Parak F., Young R. D., *Annu. Rev. Biophys. Chem.*, 1988, 17, 451; (b) Traylor T. G., *Pure Appl. Chem.*, 1991, 63, 265.
- ⁴¹ Proniewicz L. M., Bajdor K., Nakamoto K., *J. Phys. Chem.*, 1986, 90, 1760.
- ⁴² Hendrickson D. N., Kinnaird M. G., Suslick K. S., *J. Amer. Chem. Soc.*, 1987, 109, 1243.
- ⁴³ Bizet C., Morliere P., Brault D., Delgado O., Bazin M., Santus R., *Photochem. Photobiol.*, 1981, 34, 315.
- ⁴⁴ Bartocci C., Scandola F., Ferri A., Carassiti V., *J. Amer. Chem. Soc.*, 1980, **102**, 7067.
- ⁴⁵ Maldotti A., Bartocci C., Chiorboli C., Ferri A., Carassiti V., *J. Chem. Soc. Chem. Comm.*, 1985, 881.
- ⁴⁶ Bartocci C., Maldotti A., Varani G., Carassiti V., Battioni P., Mansuy D., *J. Chem. Soc. Chem. Comm.*, 1989, 964.
- ⁴⁷ Maldotti A., Bartocci C., Amadelli R., Carassiti V., *J. Chem. Soc. Dalton Trans.*, 1989, 1197.
- ⁴⁸ Bartocci C., Maldotti A., Varani G., Battioni P., Carassiti V., Mansuy D., 1991, in press.
- ⁴⁹ Ferri A., Bortolotti F., *Inorg. Chim. Acta*, 1986, 125, 129.
- ⁵⁰ Bartocci C., Maldotti A., Carassiti V., Traverso O., Ferri A., *Inorg. Chim. Acta*, 1985, 107, 5.
- ⁵¹ Bartocci C., Maldotti A., Traverso O., Bignozzi C. A., Carassiti C., *Polyhedron*, 1983, **2**, 97.
- ⁵² Bartocci C., Amadelli R., Maldotti A., Carassiti V., *Polyhedron*, 1986, **5**, 1297.
- ⁵³ Maldotti A., Varani G., Amadelli R., Bartocci C., Ferri A., *New. J. Chem.*, 1988, 12, 819.
- ⁵⁴ Rehorek D., Berthold T., Hennig H., Kemp T. J., *Z. Chem.*, 1988, **28**, 72.
- ⁵⁵ Richman R. M., Peterson M. W., *J. Amer. Chem. Soc.*, 1982, 104, 5795.
- ⁵⁶ Peterson M. W., Rivers D. S., Richman R. M., *J. Amer. Chem. Soc.*, 1985, **107**, 2907.
- ⁵⁷ Guest C. R., Straub K. D., Hutchinson J. A., Rentzepis P. M., *J. Amer. Chem. Soc.*, 1988, **110**, 5276.
- ⁵⁸ Peterson M. W., Richman R. M., *Inorg. Chem.*, 1985, **24**, 7222.
- ⁵⁹ This work was supported by the National Institute of Health. We gratefully acknowledge receipt of an N.I.H. Research Career Development Award (K.S.S.) and an N.I.H. Traineeship (R.A.W.).